

Influence of Inert Gas Dilution on Soot Formation in Laminar Non-premixed Methane Flames studied by LII

A. Flügel, J. Kiefer*, A. Leipertz

Lehrstuhl für Technische Thermodynamik (LTT) & Erlangen Graduate School in Advanced Optical Technologies (SAOT), Universität Erlangen-Nürnberg, Am Weichselgarten 8, D-91058 Erlangen, Germany

Abstract

In this work laser-induced incandescence has been employed in laminar methane diffusion flames at atmospheric pressure in order to study the influence of adding inert gas on the soot formation. A co-axial burner stabilized with co-flow air was used to produce a laminar non-premixed methane flame with constant methane mass flow. The fuel was diluted with nitrogen. Laser-induced incandescence was generated by a frequency-doubled pulsed Nd:YAG laser. The experimental results show that at constant measurement location the soot concentration as well as the primary soot particle diameter decreases with adding nitrogen.

1. Introduction

Soot is a term used for carbonaceous nanoparticles typically formed from incomplete combustion of hydrocarbons. Combustion generated soot is of particular importance in many areas in combustion research and technology. There are applications where soot formation is wanted, e.g., in the production of carbon black or when heat should be carried away from the combustion process by thermal radiation. In other applications the formation of soot should be avoided as it is a pollutant, e.g., in automotive and industrial exhaust gases. In addition to the elemental carbon, the soot particles normally contain polycyclic aromatic hydrocarbons (PAH) which act as precursors in the soot formation process and are human carcinogens. For this reason and also due the incomplete combustion, the soot formation has been studied as one of the most serious challenges to combustions researchers and engineers. In order to understand the formation and oxidation of soot many attempts have been made in the past using either modeling approaches based on physical and chemical fundamentals or diagnostic approaches allowing the experimental investigation of fundamental and real processes.

In general, on the one hand the tendency of a flame to form soot is strongly dependant on the fuel or rather the fuel composition. On the other hand the flame type (premixed, partially premixed or non-premixed) plays a key role. In the latter respect diffusion flames are often mentioned to be sooty [1, 2]. Moreover, fuel additives, e.g., inert gases can influence the sooting behavior significantly.

Various experiments have been conducted in laminar diffusion flames adding inert gas and other fuels with the purpose to study the influence of transport properties on the soot formation mechanism [3-6]. The investigations in this field showed that the reduction of the soot results from three possible phenomena: (1) the effect of mixture dilution between gas and fuel results in changing in the amount of carbon per unit of weight [7, 8]; (2) a thermo-effect due to changing the flame

temperature [9] and (3) soot reduction through the chemical interaction due to the changing of the combustion boundary conditions [3, 4, 10].

Concerning diagnostics laser-induced incandescence (LII) is an established tool capable to determine soot concentration and particle size in principle in real time. Therefore it is well suited for the investigation of the formation and destruction processes of soot particles in flames. A high energetic laser pulse is send through a flame and part of the energy is absorbed by the soot particles which are heated up as a result. Subsequently, i.e. after the laser pulse, the soot particles cool down again mainly caused by sublimation and heat conduction. In LII the temporal evolution of the Planck radiation is recorded containing the information about particle size and soot mass concentration.

2. Specific Objectives

In this work time-resolved laser-induced incandescence has been employed in an atmospheric pressure laminar methane diffusion flame in order to study the local change in soot formation with adding inert gas in terms of nitrogen.

3. Laser-Induced Incandescence

The fundamentals of LII have been discussed in detail in a number of books and review articles, see e.g. [11-13] and the references therein. Its basic principle is the rapid heating of nanoparticles up to their sublimation temperature within a few nanoseconds by irradiating a short highly intense laser pulse, and the subsequent detection and evaluation of the enhanced thermal radiation according to Planck's law. During the cooling down of the particles the heat loss is dominated by different mechanisms, mainly sublimation and heat conduction. The contribution of the thermal radiation to the energy loss is comparatively small at all times.

By employing a fast photomultiplier tube for the detection of the LII signal the time-resolved cooling process of the particles can be traced yielding information about the particle mass concentration as

* Corresponding author: jk@ltt.uni-erlangen.de

well as the particle size distribution. The LII signal and the microphysical processes can be better understood by introducing the energy balance of an isolated particle as it is given in Eq. 1.

$$\underbrace{\frac{dE_{\text{abs}}}{dt}}_{\text{Absorption}} - \underbrace{\Lambda(T_p - T_G)\pi d_p^2}_{\text{Heat Conduction}} + \underbrace{\frac{\Delta H_s}{M_g} \frac{dm}{dt}}_{\text{Sublimation}} - \underbrace{\pi d_p^2 \int \varepsilon(d_p, \lambda) M_\lambda^b(T, \lambda) d\lambda}_{\text{Thermal Radiation}} = \underbrace{\frac{dE_{\text{int}}}{dt}}_{\text{Energy difference}} \quad (1)$$

The temporally resolved particle temperature can be calculated by solving the differential equation including the laser absorption dE_{abs}/dt , the Knudsen number dependent heat transfer coefficient Λ , the particle temperature T_p and diameter d_p , the temperature T_0 of the surrounding gas, the sublimation enthalpy ΔH_s , the molar mass M_g , the mass loss owing to sublimation dm/dt and thermal radiation (emission coefficient ε , spectral energy density M_λ^b , wavelength λ) according to Planck's law, as well as the change of the internal energy dE_{int}/dt . Thereby, the equation given above includes the assumption of spherical primary particles (diameter d_p), which have only point contact to other particles inside the aggregates, therefore heat conduction between particles can be neglected. Eventually, the detectable signal can be determined by applying Planck's radiation law.

When high laser pulse energies are employed sublimation becomes the dominating mechanism and Eq. 1 reduces to Eq. 2

$$\frac{\Delta H_s}{M_g} \frac{dm}{dt} = \frac{dE_s}{dt} \quad (2)$$

showing that the energy loss due to sublimation, dE_s/dt , is proportional to the enthalpy (ΔH_s) and mass variation, dm/dt . For this reason it is possible to

calculate the soot concentration from the max signal. At later times after the laser pulse the heat conduction term of Eq.1 becomes dominating and the signal time decay can be calculated in dependence on the primary particle

diameter

$$-\frac{6\Lambda(T - T_G)}{d_p \rho_s c_p} = \frac{dT}{dt} \quad (3)$$

where T and T_G are respectively environment and gas temperature, ρ_s is soot density, Λ heat transfer coefficient and c_p specific heat capacity. Further details can be found in Refs. [14, 15].

In short, at later times after the laser pulse heat conduction to the ambient gas is the dominant heat loss mechanism and so particles with diverse specific surface area cool down differently. From the temporal signal decay the primary particle size can be derived, while the signal maximum is proportional to the mass concentration.

4. Experiments

The experiment was carried out in an atmospheric pressure laminar methane diffusion flame on a Bunsen type burner stabilized by an axial-symmetric co-flow of air. The nitrogen diluted methane fuel was supplied through an 18 mm diameter tube (820 mm long), the co-flow tube had about 40 mm diameter. Shown on the right hand side of Fig. 1 is the schematic of the burner and a detailed description can be found in reference [16]. The gas flow rates were controlled by mass flow

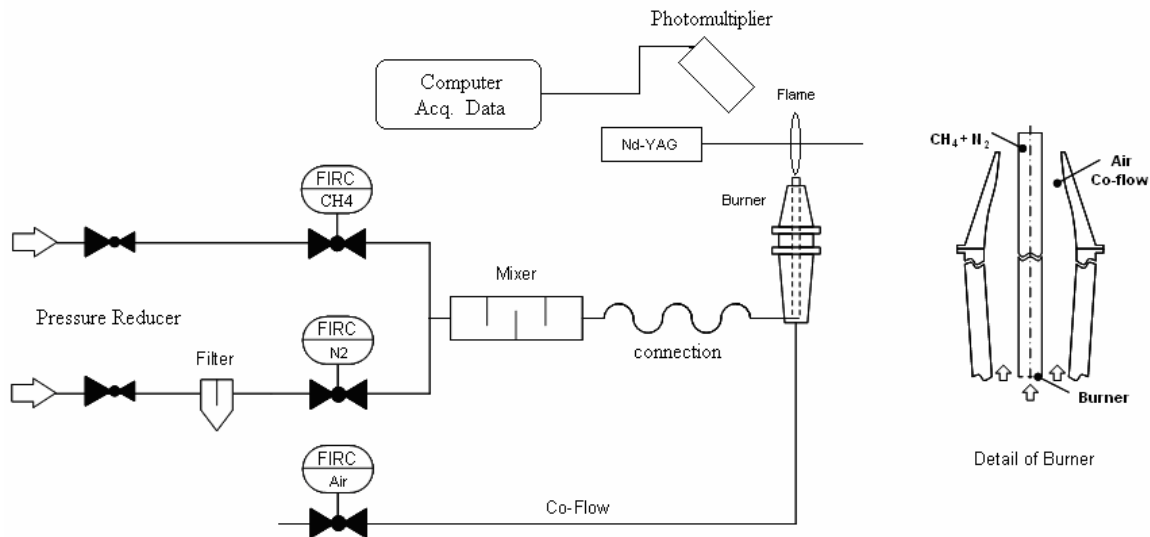


Fig. 1: Schematic of the experimental setup on the left side and detail of the Haumann burner on the right side.

controllers (Bronkhorst F-210EV). The methane and air flow rates were kept constant at 0.023 g/s and 0.4 g/s, respectively. The nitrogen mass flow rate was varied from 0 to 0.028 g/s in steps of ~ 0.002 g/s at the standard condition. The N_2 was premixed with the CH_4 in a T-mixer after the mass flow controllers and it reached the combustion zone with a laminar and homogeneous flow profile. The resulting visible flame height was about 320 mm. It should be mentioned that adding a higher amount of nitrogen than 0.028 g/s led to extinction of the flame.

Laser-induced incandescence was used to measure the soot variation. A pulsed, frequency-doubled Nd:YAG laser at a wavelength of 532 nm with a pulse duration of 9 ns was used as an excitation light source and the collimated Gaussian beam crossed the flame centre at a height of 200 mm above the burner exit. The mean laser power density was approximately 10^8 W/cm². Elastically scattered light was filtered with a Notch filter (532 nm) and the LII signal was eventually detected by a photomultiplier tube (Hamamatsu). A detailed schematic of the experimental setup is illustrated in Fig. 1.

5. Results and Discussion

Photographs of the laminar diffusion flames under investigation are displayed in Fig. 2. The pictures were taken with a commercial CCD camera without spectral filters. In order to be able to obtain accurate flame heights the picture of a calibrated grid was taken before the flame was installed. The photo to the very right presents the flame in its basic state, i.e., without

addition of nitrogen gas to the methane fuel. The flame shows a bright yellow intensity, which indicates great formation of soot in a wide flame region. The visible flame height fluctuated moderately 320 ± 20 mm. Interestingly, all flames showed approximately the same total visible height around 320 mm. The tip of the visible sooting region showed slight fluctuations because the air co-flow could not stabilize the flame at heights bigger than 250 mm above the burner exit. However, the measurement volume was positioned at 200 mm where the flame instabilities were negligible. The pictures which show the natural flame emissions are dominated by the strong incandescence of the soot particles, but the luminosity of the sooty region strongly decreased with adding nitrogen. Moreover, the lower, blue flame zone where the chemiluminescence of intermediate radical species dominates becomes larger with the amount of added inert gas. The increase of nitrogen concentration in the fuel gas dilutes the flame causing a fall of temperature and a change in the flame chemistry. As a result soot is formed at upper locations only and the flame changes its appearance. The same behaviour was observed already in the 1960s in laminar ethylene diffusion flames [17]. The thermal diffusivity of an added gas has influence on the temperature distribution, which in turn can reduce the tendency of soot formation in a diffusion hydrocarbon flame [2]. This dilution effect of an inert gas has a directly proportional influence on the soot volume fraction; the temperature gradient, hence the altering of thermal diffusivity reduces considerably the soot formation [18]. These effects can in principle be seen from the flame

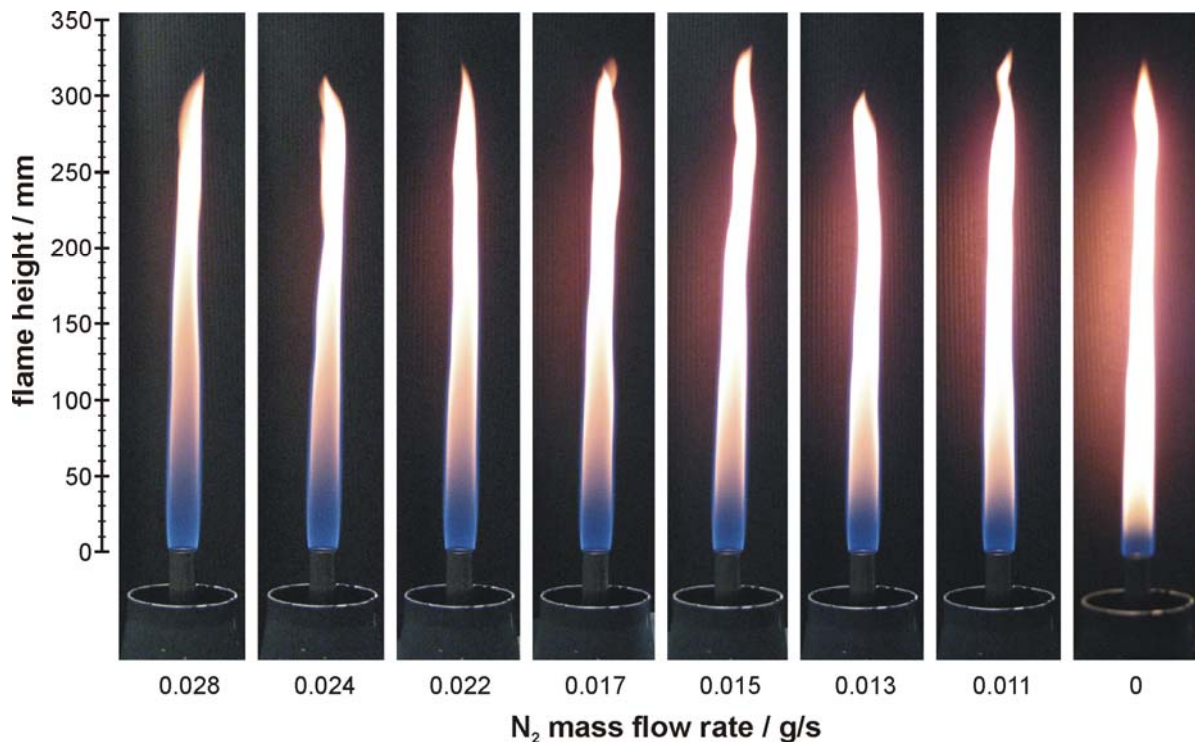


Fig. 2: Effect of nitrogen addition to the diffusion methane flame. Below each photo are the nitrogen flow rates added to the fuel.

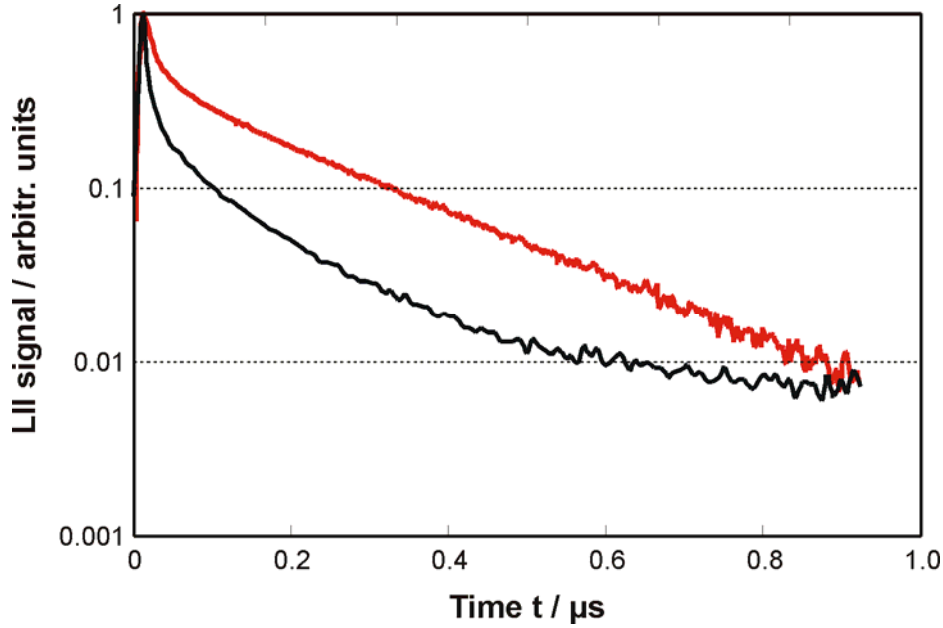


Fig. 3: Experimental LII signal from the undiluted (red line) and a nitrogen diluted (black line) methane diffusion flame.

pictures in Fig. 2.

Nevertheless, the LII measurements provide a more accurate and quantitative picture of the inert gas influence on the soot formation. The detected time-resolved LII signal from the undiluted flame is shown in Fig. 3 on a log-scale after dividing the entire signal trace by the max value of the curve. In principle, during the laser pulse, the soot particles absorb the light energy and reach their maximal temperature of about 4000 K. Subsequently, the particles cool down slowly in accordance to their specific size: bigger particles cool down slowly owing to their small surface/volume ratio, for small particles it is vice versa. Through the time exponential decay it is possible to calculate the primary particle size. At times after 150 ns the signal shape is almost perfectly linear in the log diagram indicating an exponential decay from a fairly mono-disperse particle size distribution. In addition, the normalized signal is displayed in Fig.3 for the case of dilution with 0.013 g/s nitrogen as an example. The signal temporal shape changed completely in the diluted flame not showing linear decay behaviour any more. This clearly indicates a broader primary particle size distribution compared to the undiluted flame. The same holds for the other diluted flame cases which are not displayed for clarity reasons. Moreover, the decay between 150 ns and 450 ns appears much faster in the diluted flame indicating that a substantial amount of the entire soot has a smaller primary particle size. This conclusion is supported by the results of the studies discussed in the Introduction. When the hydrocarbon fuel is diluted with a non-hydrocarbon gas the probability of collisions between the different soot precursor molecules is smaller hence the particle growth is hindered. A

summary of the derived mean decay times is given in Table 1 for all flames investigated. The trend of decreasing decay time with increasing nitrogen dilution indicates that the mean primary particle diameter decreases with adding inert gas.

Furthermore, the LII signal intensity yields an estimate for the soot mass concentration. In order to allow an easy comparison of the individual measurements, the factor of mass concentration, F_{MC} , is introduced as a quantity being proportional to the measured signal intensity hence being also proportional to the soot concentration. The numbers derived from the experimental LII signals are summarized in Table 1. The highest LII signal intensity was observed in the undiluted methane flame. This is in good agreement with the flame photographs discussed beforehand. With adding nitrogen the max signal intensity significantly decreases indicating lower soot concentrations. The data shown in Table 1 is plotted in Fig. 4 in order to allow a direct overview and comparison.

The signal decay times decrease exponentially with nitrogen mass flow rate while the signal decay time decreases linearly indicated by best fit exponential and linear curves (solid lines), respectively.

In general, the soot particle sizes and concentrations change significantly when nitrogen is added. The results are in agreement with simulated data from laminar ethylene diffusion flames, where the influence of transport properties on soot formation was numerically analyzed considering injection of inert gas in the fuel stream [19]. The temperature profile modifies causing a concentration change due to the mass diffusion variation and therefore produces modification on the soot yield.

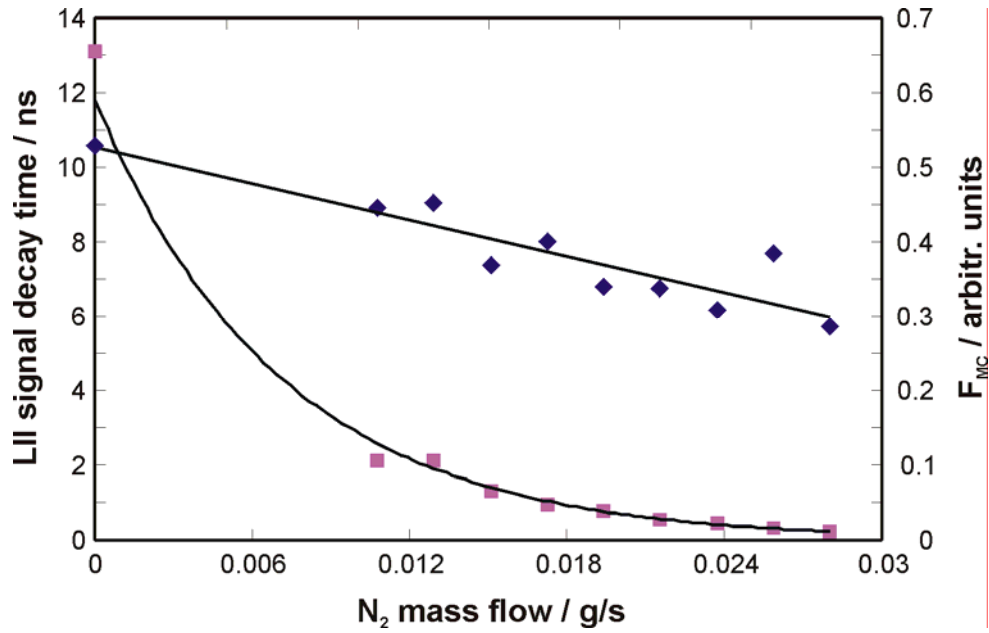


Fig. 4: LII signal decay time (diamonds) and mass concentration factor (squares) as functions of nitrogen dilution mass flow rate.

Tab. 1: N_2 flow, decay time and mass concentration factor F_{MC} .

| N_2 flow rate in [g/s] | decay time in [ns] | F_{MC} |
|-----------------------------|-----------------------|----------|
| 0.028 | 5.72 | 0.011 |
| 0.026 | 7.71 | 0.016 |
| 0.024 | 6.18 | 0.022 |
| 0.022 | 6.73 | 0.028 |
| 0.019 | 6.8 | 0.039 |
| 0.017 | 8.02 | 0.048 |
| 0.015 | 7.39 | 0.066 |
| 0.013 | 9.03 | 0.106 |
| 0.011 | 8.93 | 0.106 |
| 0.000 | 10.6 | 0.655 |

6. Summary and Conclusion

In this work we analyzed the influence of adding inert gas in the fuel stream of a methane diffusion flame on the formation of soot particles. The experiments using laser-induced incandescence, LII, were performed in laminar diffusion flames stabilized with an air co-flow. The nitrogen mass flow rate was systematically varied. Interestingly, the flame height remained almost constant at all flame conditions. The time-resolved LII signal was detected by a photomultiplier tube. Both the total signal intensity giving an estimate for the soot concentration as well as the signal decay time indicating the primary particle size decreased with increasing nitrogen mass flow at constant methane mass flow rate. The dependence of the soot concentration on the nitrogen flow rate showed an exponential behavior while the LII signal decay decreased linearly with

nitrogen flow. Furthermore, the temporal shape of the LII signals indicate a fairly mono-disperse particle size distribution in the undiluted flame and, in contrast, a broad distribution when nitrogen is added.

Acknowledgement

The authors gratefully acknowledge financial support for parts of the work by the German Research Foundation (DFG) and for funding the Erlangen Graduate School in Advanced Optical Technologies (SAOT) within the framework of the German Excellence Initiative.

References

- [1] B. Atakan, H. Böhm, K. Kohse-Höinghaus, Fuel-rich chemistry and soot precursors, in K. Kohse-Höinghaus, J. B. Jeffries (eds.), Applied Combustion Diagnostics, Taylor & Francis, New York, 2002.
- [2] K.P. Schug, Y. Manheimer-Timnat, P. Yaccarino, I. Glassman, Combust. Sci. Technol. 22 (1980) 235.
- [3] Ö.L. Gülder, D.R. Snelling, Combust. Flame 92 (1993) 115-124.
- [4] Ö.L. Gülder, Combust. Flame 92 (1993) 410-418.
- [5] C.S. McEnally, L.D. Pfefferle, Combust. Flame 112 (1998) 545-558.
- [6] C.S. McEnally, L.D. Pfefferle, Combust. Flame 115 (1998) 81-92.
- [7] I. Glassman, Combustion, 1st ed., Academic Press Inc., Orlando, 1977.
- [8] D.X. Du, R.L. Axelbaum, C.K. Law, Combust. Flame 102 (1995) 11-20.

- [9] C. Wey, Proceedings of the SPIE 2122 (1994) 94-106.
- [10] D.X. Du, R.L. Axelbaum, C.K. Law, Proc. Combust. Inst. 23 (1990) 1501-1507.
- [11] R.J. Santoro, C.R. Shaddix, Laser-induced incandescence, in K. Kohse-Höinghaus, J. B. Jeffries (eds.), Applied Combustion Diagnostics, Taylor & Francis, New York, 2002.
- [12] A. Leipertz, R. Sommer, Time-resolved laser-induced incandescence (TIRE-LII), in J. Li (eds.), Advances in Chemical Engineering, Elsevier, 2009.
- [13] H.A. Michelsen, F. Liu, B.F. Kock, H. Bladh, A. Boiarciuc, M. Charwath, T. Dreier, R. Hedef, M. Hofmann, J. Reimann, S. Will, P.-E. Bengtsson, H. Bockhorn, F. Foucher, K.-P. Geigle, C. Mounaim-Rousselle, C. Schulz, R. Stirn, B. Tribalet, R. Suntz, Appl. Phys. B 87 (2007) 503-521.
- [14] S. Will, S. Schraml, A. Leipertz, Proc. Combust. Inst. 26 (1996) 2277-2284.
- [15] S. Schraml, S. Dankers, K. Bader, S. Will, A. Leipertz, Combust. Flame 120 (2000) 439-450.
- [16] J. Haumann, A. Leipertz, Appl. Opt. 24 (1985) 4509-4515.
- [17] I.S. McLintock, Combust. Flame 12 (1968) 217.
- [18] I. Glassman, Proc. Combust. Inst. 27 (1998) 1589-1596.
- [19] H. Guo, F. Liu, G.J. Smallwood, Ö.L. Gülder, Proc. Combust. Inst. 29 (2002) 2359-2365.